Available online at www.sciencedirect.com

ScienceDirect

Solar Energy 122 (2015) 347–358

SOLAR ENERGY

www.elsevier.com/locate/solener

Dynamic programming and Munkres algorithm for optimal photovoltaic arrays reconfiguration

Eleonora Riva Sanseverino [a], Thanh Ngo Ngoc [a,b], Marzia Cardinale [a], Vincenzo Li Vigni [a], Domenico Musso [a], Pietro Romano [a], Fabio Viola [a,*]

[a] *DEIM, University of Palermo, Palermo, Italy*
[b] *Electric Power University, HaNoi, Viet Nam*

Received 4 February 2015; received in revised form 2 September 2015; accepted 3 September 2015

Communicated by: Associate Editor Nicola Romeo

Abstract

In this paper, an original formulation of the control problem for optimal PV array reconfiguration, following a Total Cross Tied layout, is proposed. The formulation follows the well-known subset sum problem, which is a special case of the knapsack problem. The reconfiguration is a measure devoted to mitigate the mismatch effect and maximize the output power of small photovoltaic plants under non-homogeneous working conditions. Therefore, reconfiguration means changing the connections of the solar panels adaptively by a dynamic switching matrix. The control system implements an easy dynamic programming algorithm to change the switches layout.

The use of the Munkres assignment method in a post-processing module makes the algorithm able to obtain the optimum configuration for which it is possible to balance and minimize the aging of the switches within the switching matrix.

Keywords: Mismatch; Photovoltaic modules; Optimization; Reconfiguration

1. Introduction

In the last years, global warming and energy policies have become a hot topic on the international agenda. Developed countries are trying to reduce their greenhouse gas emissions. The European Union has committed to reduce the emissions of greenhouse gas to at least 20% below the level in 1990, and to produce more than 20% of its energy consumption from renewable sources by 2020. In this context, the photovoltaic (PV) power generation plays an important role due to the fact that it is a green source. The only emissions associated with the PV power generation are those from manufacturing of solar PV components. After their installation, they generate electricity from the solar irradiation without emitting greenhouse gases. In their lifetime, which is around 25 years, PV panels produce more energy than that needed for their manufacturing (MacKay, 2009). In addition, they can be installed in places with no other use, such as roofs and deserts, and they can produce electricity for remote locations, where there is no electrical grid. The latter type of installations is known as off-grid facilities and sometimes they are the most economical alternative to provide electricity in isolated areas. However, most of the generated PV power comes from grid-connected installations, where the power

* Corresponding author.
E-mail addresses: eleonora.rivasanseverino@unipa.it (E.R. Sanseverino), thanhnn_cntt@epu.edu.vn (T.N. Ngoc), marzia_cardinale@hotmail.it (M. Cardinale), vincenzo.livigni@unipa.it (V. Li Vigni), domenico.musso@gmail.com (D. Musso), pietro.romano@unipa.it (P. Romano), fabio.viola@unipa.it (F. Viola).

http://dx.doi.org/10.1016/j.solener.2015.09.016
0038-092X/

Nomenclature

avg	sum of irradiance on the row ideal after reconfiguration
BIPV	building-integrated photovoltaic
BL	bridge-link
BWSA	best–worst sorting algorithm
DES	Dynamic Electrical Scheme
DPST	double-pole single-throw
EI	Equalization Index
g	number of panels
HC	Honey-Comb
i	row index
I–V	current–voltage
j	column index
m	number of rows
MPP	maximum power point
MPPT	maximum power point tracker
n_i	number of modules that are parallel connected of the row i
N_{PV}	number of PV modules
N_{SW}	number of switches
P	total irradiance
P–V	power–voltage
P_i	total irradiance of the row i
P_{ij}	irradiance value of module located on row i and column j
PS	partial shading
PV	photovoltaic
q	reconfigurable modules
SP	Series–Parallel array
TCT	Total-Cross-Tied
MAA	Munkres' Assignment Algorithm

is fed to the grid. It is a growing business in developed countries such as Germany which in 2013 is by far the world leader in PV power generation followed by Spain, Japan, USA and Italy (Trends in Photovoltaic Applications, 2013).

On the other hand, due to the equipment required, the PV power generation is more expensive than other resources. The Governments are promoting it with subsidies or feed-in tariffs, expecting the development of the technology so that in the near future it can become competitive (Trends in Photovoltaic Applications, 2013; Electricity from Sunlight, 2011). Increasing the efficiency in PV plants so that the generated power increases is a key aspect, as it will increase the incomes, reducing consequently the cost of the power generated and thus approaching the cost of the power produced from other sources.

However, in many applications, such as solar power plants, building-integrated photovoltaic (BIPV) or solar tents, the solar photovoltaic arrays might be illuminated non-uniformly. The causes of non-uniform illumination may be a lot, such as the shadow of clouds, trees, neighbor's houses, or the shadow of one solar array on the other. This further leads to nonlinearities in characteristics (Nguyen and Lehman, 2008).

For these new applications, it has been especially important to optimize performance of the arrays in non-homogeneous shading conditions. Because of the nature of the electrical characteristics of solar cells, the maximum power losses are not proportional to the shadow, but increase nonlinearly (Rauschenbach, 1971).

The presence of shadows over a solar PV array can cause many undesired effects:

- The power generated from the solar PV array is much less than the nominal one (Quaschning and Hanitsch, 1996).
- The local hot spot in the shaded part of the solar PV array (called partial shading) can damage the solar cells.

The shaded solar cells may work on the negative voltage region, become a resistive load, and absorb power. Bypass diodes are sometimes parallel connected to the solar cells in order to protect them from damage. However, in most cases, just one diode is parallel-connected to a group of solar cells (Swaleh, 1982) and this hides the potential output power of the array.

In Achim Woytea and Belmans (2003) and El-Dein et al. (2012) the power losses due to partial shading (PS) is given. Different losses induced by PS are shown in Fig. 1, where the maximum possible power under PS is the sum of the maximum powers of the individual modules when operating independently under the same irradiance levels dictated by array PS.

The maximum possible power is not equal the array maximum power without partial shading. The difference is the shading losses, which cannot be invalidated.

Operative techniques for declining partial shading losses could be grouped into the following main three categories (El-Dein et al., 2012):

- Distributed maximum power point tracker (MPPT).
- Multilevel inverters.
- Photovoltaic array reconfiguration.

The first two issues have been treated extensively in the technical literature, and it is not the intention of this article to expand the state of the art or make a comparison of the efficiency of different systems. The reconfiguration is an efficient rearrangement of connections of PV modules in order to ensure the maximization of the power, but also the operation of the inverter. The current state-of-the-art strategies for photovoltaic array reconfiguration utilizing

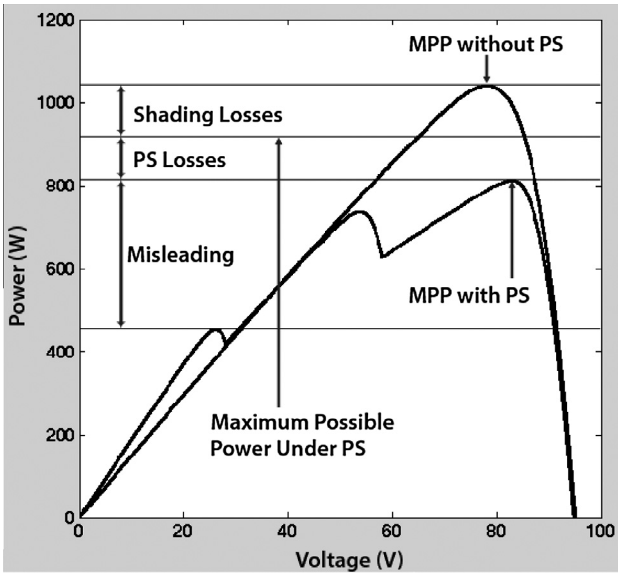

Fig. 1. Shading, partial shading, and misleading losses for a photovoltaic array.

the "irradiance equalization" principle are extensively reviewed in La Manna et al. (2014).

In this paper, an original formulation of the control problem for optimal PV array reconfiguration, following a Total Cross Tied layout (TCT), is proposed.

2. Reconfiguration strategy

The reconfiguration strategy can be applied to two different typical environmental situations; firstly, when the plant is affected by the shadow, which is projected by a fixed object. This is common for PV plants, which are placed on the roof or integrated in a building. In general, the technicians should avoid placing PV modules where a fixed object (i.e., a chimney) can project a shadow during the day. In the event of failure of one or many modules, these can be automatically disconnected by the reconfigurable array. Secondly, when a portion of a large PV plant is affected by passing clouds. In this case, there is generally a distributed drop of irradiance above all the PV plant. Depending on the speed of the passing clouds, the irradiance conditions can change suddenly, giving rise to a large deterioration of the PV plant efficiency.

Many challenging aspects, influencing the control chain as depicted in Fig. 2, influence the design of dynamic reconfiguration systems that can cope with environmentally variable conditions, shadings or failures both in small likewise in larger plants.

The *data acquisition* is executed through suitable measurement devices allowing to collect the field data required for the *PV mathematical model* providing input data for the *reconfiguration* algorithm. The latter two make up an open loop control system and therefore the more accurate the PV mathematical model, the best control actions the reconfiguration system will give to the actuator. The *switching matrix* is the actuator. It implements the desired *optimal configuration* of the PV plant. In the following sections, each of the cited elements of the control chain will be particularized.

As far as the *reconfiguration* algorithm is concerned, some interesting optimization algorithms for irradiance equalization have been proposed in the literature. As it will be shown in later sections, the *best worst sorting* algorithm (BWSA) produces largely sub optimal solutions. In Romano et al. (2013) a *random-search algorithm* (RSA) is compared to a *deterministic* approach. Even if the random search algorithm is fast, it may give different results starting from the same input data due to the inherent randomness of the method. Moreover, none of the proposed algorithms accounts for the aging of the relays employed in the reconfiguration system.

This paper shows an original formulation of the control problem for optimal PV array reconfiguration, following a Total Cross Tied layout (TCT). The flowchart of the algorithm implementing this reconfiguration strategy is show in Fig. 3. The formulation follows the well-known subset sum problem, which is a special case of the knapsack problem. The *reconfiguration* algorithm is a dynamic optimization algorithm, then the use of the *Munkres' Assignment* Algorithm (MAA) (Munkres, 1957) allows to obtain a solution with a minimum number of switching operation, so as to preserve the lifetime of the switching matrix. In this way, the maximization of the output power of PV generation system under non-homogeneous solar irradiation is obtained.

2.1. Connection topologies of PV array

Many alternative array interconnection topologies have been proposed for reducing mismatch losses (Ramaprabha, 2012; Ramabadran, 2009; Ramaprabha et al., 2010; Ramaprabha and Mathur, 2008; Picault et al., 2010; El-Dein et al., 2011; Villa et al., 2012; Tian et al., 2013; Liu et al., 2014; Lorente et al., 2014), they include Series array (Fig. 4a), Parallel array (Fig. 4b), Series–Parallel array (SP)

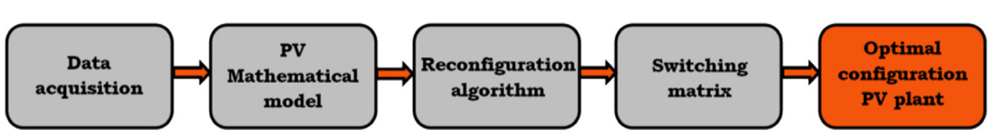

Fig. 2. Dynamic reconfiguration system for PV plant: flow chart for optimal design (La Manna et al., 2014).

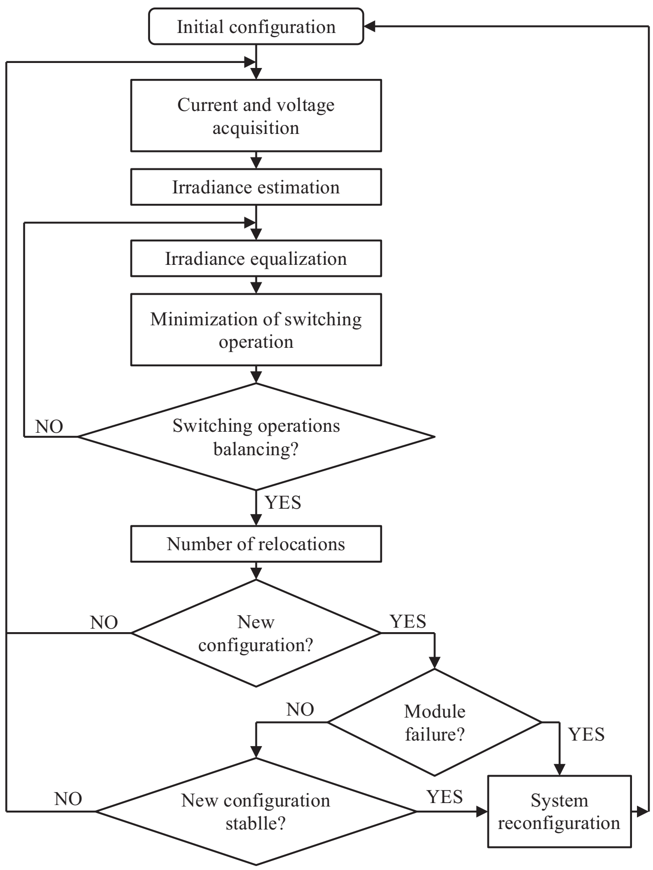

Fig. 3. Flowchart of the algorithm for the system reconfiguration.

(Fig. 4c), total-cross-tied (Fig. 4d), bridge-link (BL) (Fig. 4e) and Honey-Comb (HC) (Fig. 4f). Moreover the advantages and disadvantages of each method are explained (La Manna et al., 2014). Solar modules are connected in series in order to increase the total voltage and in parallel to increase the total current.

Although many convenient interconnection topologies have been developed, so far the most exploited solutions rely on SP and TCT module interconnections.

2.2. Reconfiguration for TCT topology

As already discussed in La Manna et al. (2014), the TCT interconnection allows to decrease the overall effects of mismatch. With TCT interconnection, it can be concluded as follows:

- The maximum power point (MPP) voltage of parallel-connected PV modules will not be greatly affected by the value of the irradiance on each module.
- The current flowing through a set of parallel-connected PV modules will be almost proportional to the quantity of the irradiance values present on each module.

The challenge in a TCT reconfiguration technique consists in connecting PV modules in irradiance-balanced tiers. In Velasco-Quesada et al. (2009), the equalization index principle is proposed. As it will be detailed right below in this section, irradiance equalization aims to obtain series connected tiers, also called rows, where the sum of the irradiances of the modules is the same; this results in a string where the circulating current is proportional to the given sum of irradiances of one row. The algorithm equalizes the available power on each row, thus some ideal current generators, with the same nominal values, are connected in the string, avoiding mismatch losses.

Indicating with P_{ij} the irradiance value of the module located on row i and column j within the topology shown in Fig. 7. The total irradiance of the row i, P_i, is defined as

$$P_i = \sum_{j=1}^{n_i} P_{ij} \tag{1}$$

where n_i is the number of modules that are parallel connected of the row i. For each configuration, the algorithm calculates the Equalization Index (EI) by means of the following expression:

$$\mathrm{EI} = max_i(P_i) - min_i(P_i) \quad \forall i \tag{2}$$

This index quantifies the level of current limitation of the configuration and thus the one minimizing EI is selected. The secondary target followed by the algorithm is the smallest number of switching operations starting from the initial configuration to the optimized configuration.

Under the same equalization index, the configuration with the least number of switching operations to be performed is selected.

The example reported in Fig. 5 clarifies the issue.

Fig. 5 shows that, in (a), the rows have different irradiance levels: 2300 W/m^2, 1800 W/m^2 and 1300 W/m^2 respectively; in (b), changing the PV modules position following a reconfiguration approach (modules 1 have been switched from row 1 to row 3), the irradiance is equalized to 1800 W/m^2 in all rows. The MPP before reconfiguration corresponds to 811.9 W with a misleading effect on the MPP tracking algorithm (c) while after reconfiguration it gets to 1041 W with a single maximum curve and without the misleading effect to the MPP tracking algorithm (d).

2.3. Switching matrix design

In case of non-homogeneous irradiance, the series-connection of modules with similar irradiance produce a generated power increase (Romano et al., 2013). In Romano et al. (2013), the authors introduce a fully reconfigurable Dynamic Electrical Scheme (DES) for PV generators. DES basic layout is composed by a series-connection of parallel-connected modules; this layout is usually called TCT and it is shown in Fig. 6. The DES requires a number of switches N_{SW}, which is equal to:

$$N_{\mathrm{SW}} = (2mN_{\mathrm{PV}})_{\mathrm{DPST}} + (m)_{\mathrm{SPDT}} \tag{3}$$

where DPST means double-pole single-throw switches, N_{PV} is the number of PV modules and m is the number

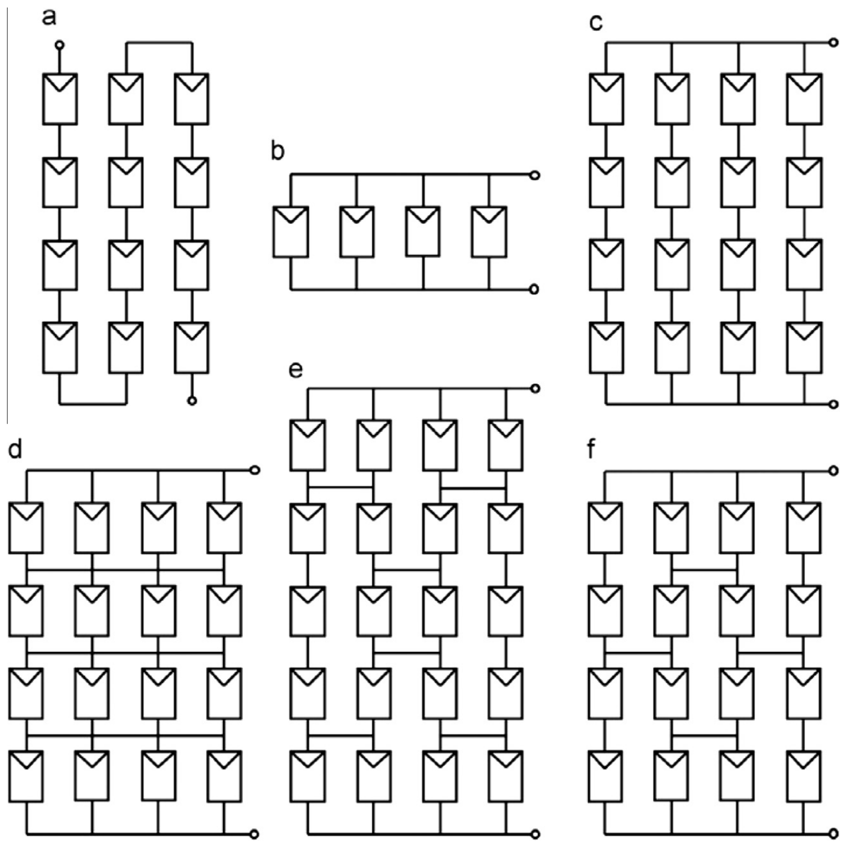

Fig. 4. (A) Series array, (b) parallel array, (c) series–parallel array, (d) total-cross tied array, (e) bridge-link array and (f) Honey-Comb array (La Manna et al., 2014).

of rows, supporting up to $(m \cdot q)!/(q!)^m$ configurations, with q reconfigurable modules.

Obviously, the DES operation must comply with the inverter input operating ranges. It is easy to get the equivalent circuit showed in Fig. 7 where a variable number of modules per row can be implemented.

3. Optimal photovoltaic array reconfiguration

The novel algorithms for optimal photovoltaic array reconfiguration is here presented. It uses the operating principle of Subset-sum problems in order to obtain the configuration that optimizes the output power. Moreover, the minimization of switching operation with Munkres' Assignment Algorithm (MAA) will be explained herein.

3.1. Overview of the problem

A TCT configuration, shown in Fig. 7, is considered. The system shows m rows and the i-th row has in general n_i modules. From now on, with P_{ij} the irradiance value of the module located on row i and column j will be indicated.

- The total irradiation of row i is defined as:

$$P_i = \sum_{j=1}^{n_i} P_{ij} \tag{4}$$

- The total irradiation P is equal to:

$$P = \sum_{i=1}^{m} P_i \tag{5}$$

- The number of modules g is equal to:

$$g = \sum_{i=1}^{m} n_i \tag{6}$$

The number of rows in which the TCT layout can be arranged m must be compatible with the inverter input voltage operating range.

In this way, the sum of irradiance on the row after reconfiguration is equal or close to

$$avg = \frac{P}{m} \tag{7}$$

4. The algorithm

As it was said before, the irradiance equalization problem can be viewed as a subset-sum problem, whose general formulation is the following: *given a set of integers and an integer s, does any non-empty subset sum to s? Subset sum can also be thought of as a special case of the knapsack problem.*

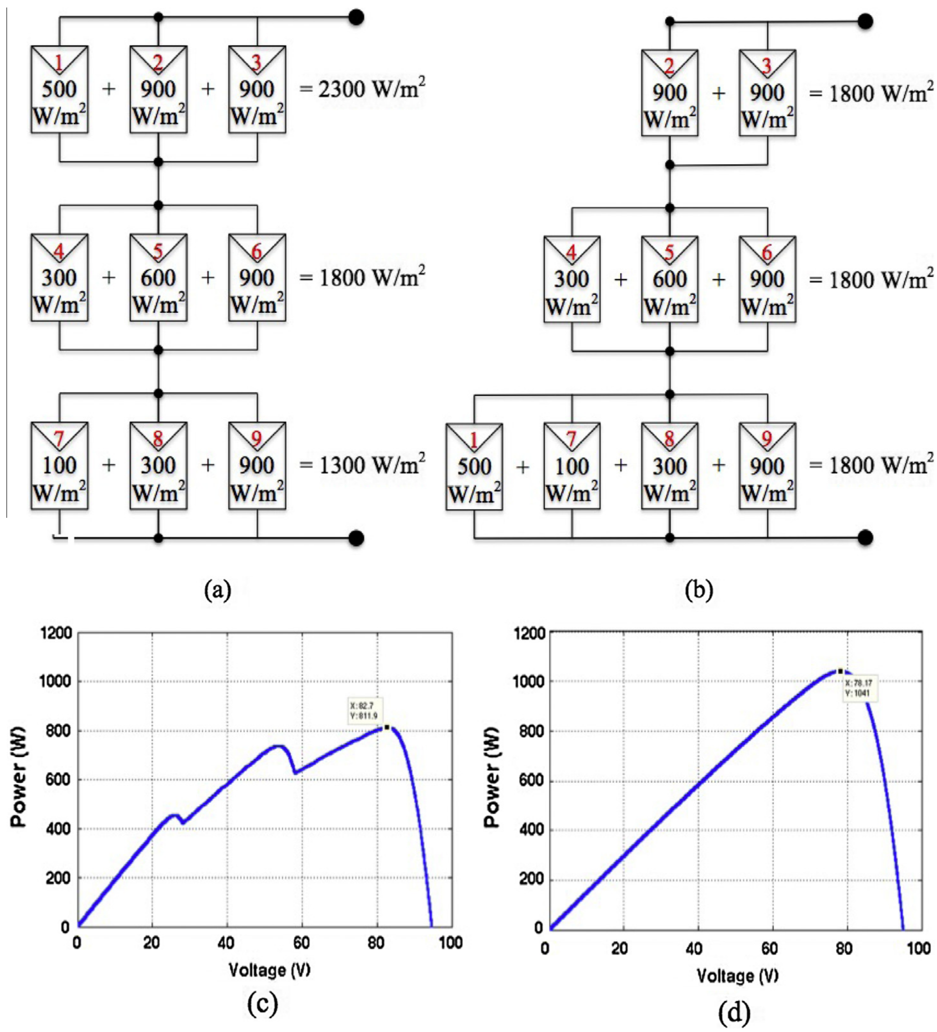

Fig. 5. Irradiance equalization example: (a) before reconfiguration, (b) after reconfiguration. MPP before reconfiguration with a misleading effect on the MPP tracking algorithm (c), after reconfiguration without the misleading effect (d).

In the problem here investigated, s is the average irradiance equal to avg as described in (7).

The proposed algorithm works as follows:

1. The value avg is first calculated as described in (7).
2. In the matrix containing the irradiance values P_{ij}, in turn the groups of elements whose irradiances sum is equal or close to avg. Each group is a row of the new matrix B.
3. Use Munkres' Assignment Algorithm to find minimum switching of modules.
4. Matrix B is suitably re-arranged.

The method is outlined in Fig. 8.

4.1. Numerical example

In what follows, a numerical example in order to clarify the algorithm steps will be illustrated.

Let us suppose to have a PV generator composed of 16 modules differently irradiated. Moreover, let us that the final TCT configuration will show four rows in order to comply with the voltage range sustained by the inverter. In the latter situation, the starting configuration could be as the one depicted in the matrix of Fig. 7. Herein the previously mentioned matrix will be named P, being P_{ij} the irradiance value of the module, located on row i and column j showed in Fig. 9.

The first step of the algorithm consists in evaluating the value of avg, which in this case is 1675 W/m^2. Then, to implement step 2, modules are sorted according to decreasing irradiance values per row and then by the first entry of each row, as shown in Fig. 10.

From now on, the latter matrix will be called A and an equivalent view of it, in vector form, is illustrated in Fig. 11.

Starting from the matrix A and from the greatest value of its first row (i.e. $A[0] = 830$), using a Subset-Sum algorithm, the first row of the new matrix, from now on called B, is obtained (see Fig. 12).

The following step consists in deleting, from the matrix A, the elements already arranged in the first row of the matrix B (see Fig. 13).

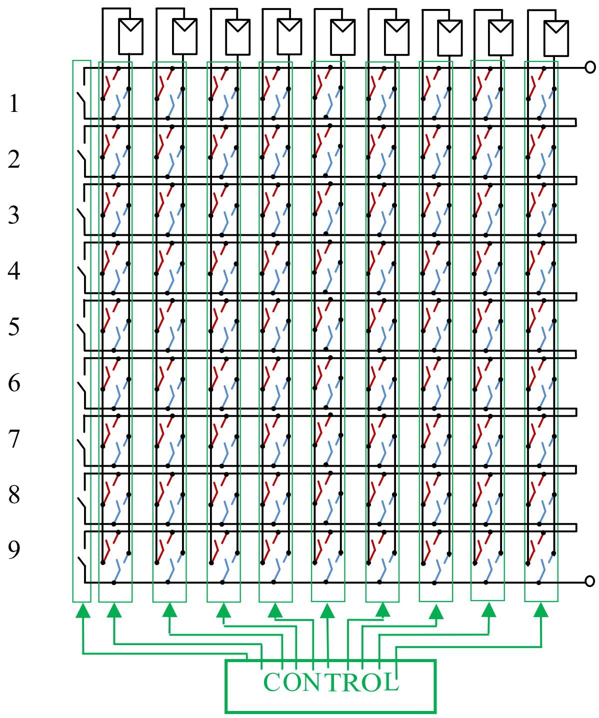

Fig. 6. Dynamic electrical scheme switching matrix (Romano et al., 2013).

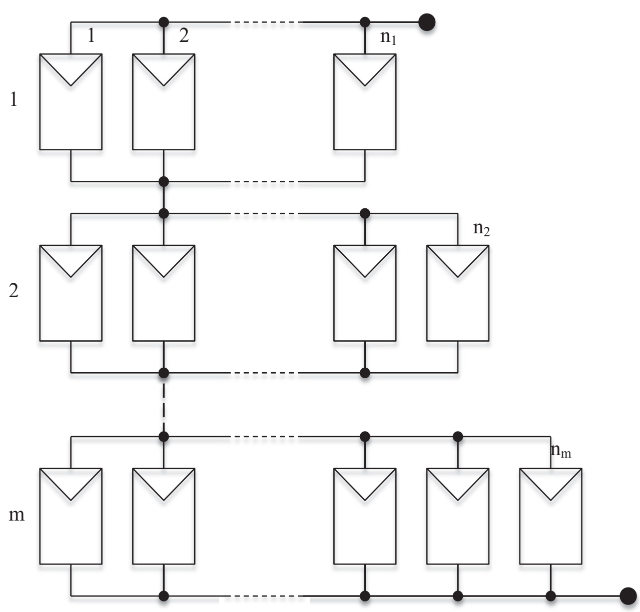

Fig. 7. Generator topology.

Then the remaining elements of the matrix A are again arranged sorted putting the greatest element in the first position, followed by all the elements pertaining to the same row (see Fig. 14). All the other elements are left in the same previous order.

Starting from the latter modified matrix A, the second row of matrix B is built by summing to the element $A[0]$ other elements in order to obtain a value equal or close to the average value 1675. By repeating the just now explained procedure until the depletion of the elements, the matrix B is obtained as shown in Fig. 15. Further information on Subset-sum problem can be found in Silvano Martello (1990).

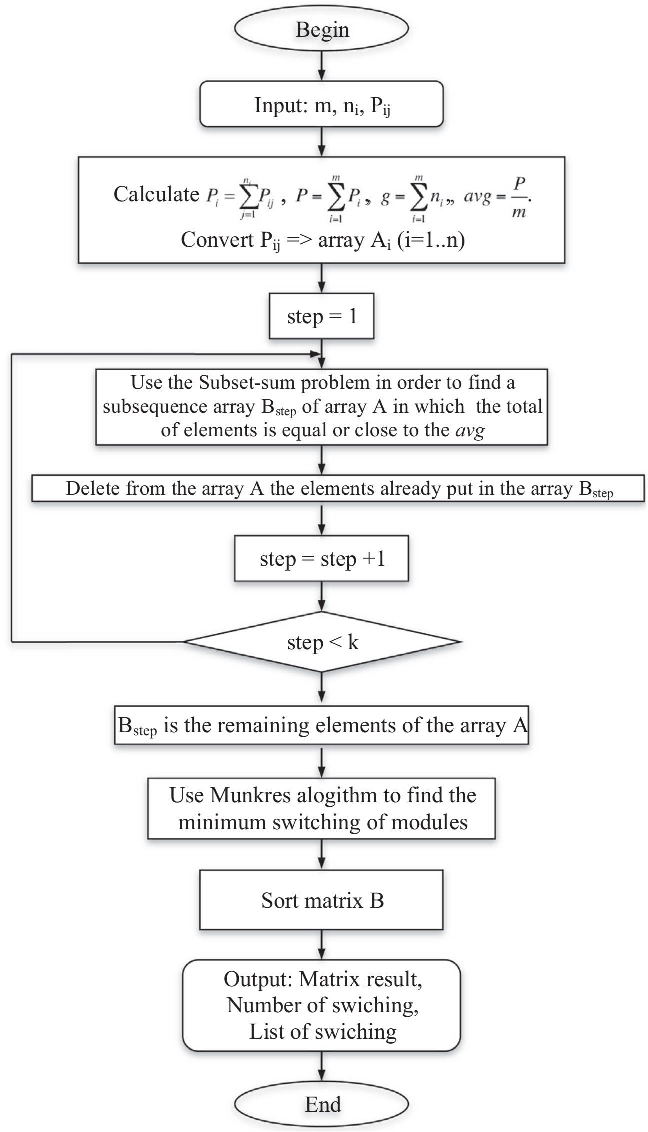

Fig. 8. Block diagram.

170	200	250	490
520	680	480	640
720	410	550	290
150	830	140	180

Fig. 9. Starting matrix P, in the entries the irradiance values in W/m^2.

830	180	150	140
720	550	410	290
680	640	520	480
490	250	200	170

Fig. 10. Sorted matrix P, in the entries the irradiance values in W/m^2.

830	180	150	140	720	550	410	290	680	640	520	480	490	250	200	170
A[0]	A[1]	A[2]	A[3]	A[4]	A[5]	A[6]	A[7]	A[8]	A[9]	A[10]	A[11]	A[12]	A[13]	A[14]	A[15]

Fig. 11. Equivalent vector view of matrix A in the entries the irradiance values in W/m^2.

550	140	150	830

Fig. 12. First row of matrix B.

550	140	150	830		**= 1670**
180	490	290	720		**= 1680**
480	520	680			**= 1680**
640	250	200	170	410	**= 1670**

Fig. 15. Intermediate matrix B.

After the determination of the matrix B, which is an intermediate matrix for our purpose, the Munkres' assignment algorithm was used.

In this way, the configuration that involves the minimum number of modules changes is implemented. In detail, on the basis of the comparison between the starting and the intermediate matrix B, the Munkres' matrix M is obtained as follows. The element M_{ij} of matrix M is a integer number that refers to the number of modules that are in the row i of the starting matrix P while they are absent in row j of the intermediate matrix B.

For better clarity, the two considered matrices are placed side by side in Fig. 16.

As an example, the entry (1,1) equals 4 because the four modules of row 1 in matrix P are different from the four modules in matrix B. The Munkres matrix M, determined as said, is shown in Fig. 17.

Taking the results of the MAA, the entries showing the minimum value on the rows are those rows in the intermediate matrix that are most similar to the starting matrix P. The final configuration is thus obtained and illustrated in Fig. 18.

As it can be observed, in the considered case the algorithm has changed the position of only five modules in order to equalize the irradiance on the rows.

5. Simulations (A2.2)

In order to prove the efficiency of the proposed algorithm, a Matlab/Simulink model was set up. The simulated control system is depicted in Fig. 19.

A PV generator with 9 identical modules with electrical characteristics described in Table 1 was implemented in a simulation environment. Modules are irradiated in a non-homogeneous way and the TCT interconnection has three rows. Fig. 20 shows the comparison between the system before and after the reconfiguration.

Before reconfiguration, the I–V (current–voltage) curve and the P–V (power–voltage) curve are shown in Fig. 20b and c with $P_{MAX} = 298.08$ W; $V_{MAX} = 26.7$ V. After reconfiguration, the PV generator is arranged as in Fig. 20d, the I–V curve and P–V curve are shown in Fig. 20e and f with $P_{MAX} = 474.8$ W; $V_{MAX} = 77.56$ V.

Moreover, the MAA will find the optimal arrangement with the smallest number of switches. In the case proposed here the MAA found the optimal configuration with only 3 switching operations. Fig. 20 shows the performance before switching (a, b, c) and after (d, e, f) (A1.1) (see Table 2).

5.1. Switching operations balancing

The described procedure is repeated a fixed number of times by using, each time, a starting value that is slightly different from the above-mentioned average value. In this way, a fixed number of sub-optimal resulting configurations is achievable. The need of having different resulting configurations resides in the aim of selecting the one involving the less used matrix switches. This approach produces a homogeneous aging of all the switches of the switching matrix, thus preserving the life span of the whole switching matrix. This aspect should not be underestimated

	180			720		410	290	680	640	520	480	490	250	200	170
A[0]	A[1]	A[2]	A[3]	A[4]	A[5]	A[6]	A[7]	A[8]	A[9]	A[10]	A[11]	A[12]	A[13]	A[14]	A[15]

Fig. 13. Matrix A after the deletion of some elements.

720	410	290	680	640	520	480	490	250	200	170	180
A[0]	A[1]	A[2]	A[3]	A[4]	A[5]	A[6]	A[7]	A[8]	A[9]	A[10]	A[11]

Fig. 14. Matrix A reordered in order to build the second row of matrix B.

170	200	250	490
520	680	480	640
720	410	550	290
150	830	140	180
Starting Matrix P			

550	140	150	830	
180	490	290	720	
480	520	680		
640	250	200	170	410
Intermediate Matrix B				

Fig. 16. Comparison between the starting and the intermediate configuration.

4	3	4	1
4	4	1	3
3	2	4	3
1	3	4	4

Fig. 17. Matrix *M*.

in view of the use of low-cost and therefore limited life span components within the switching matrix (i.e. mechanical relays). In Candela et al. (2012) the configuration performing the smallest number of modules-switching operations was chosen. Unlike this method, the approach presented in this paper moves the attention to the aging, measured in terms of number of times the switch has been used. By giving a priority to the balancing of the switches usage, it can happen that, between two suboptimal configurations, the one involving a slightly higher number of switching operations may be chosen. In Fig. 21, a PV system with 16 modules has been simulated with 300 reconfigurations, implementing the presented output power optimization. The blue columns represent the number of switching operations per module when the presented algorithm is configured for equalizing the number of switching operations of each module, basically trying to uniform the aging of the reconfiguration matrix. The red columns instead show the number of switching operations per module, when the only target is minimizing the global number of switching operations.

6. Performance comparison with other algorithms

In this section a comparison with other algorithms proposed in the literature is presented: the Electrical Array

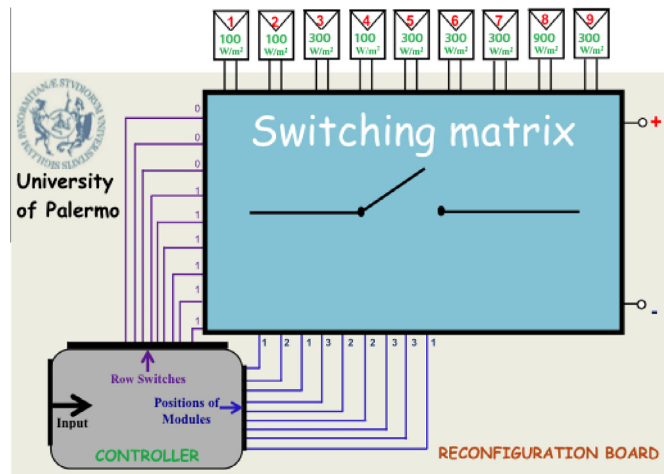

Fig. 19. Reconfiguration board.

Table 1
Electrical characteristics of PV used modules at 25 °C.

V_{MPP}	I_{MPP}	P_{MPP}	V_{OC}	I_{SC}
26.01 V	7.64 A	198 W	32.40 V	8.40 A

Reconfiguration (EAR) Velasco-Quesada et al., 2009, the BWSA used in Storey et al. (2013), the RSA and the Deterministic Algorithm proposed in Romano et al. (2013), are taken into account.

One of the biggest problems to be overcome in reconfiguration systems is the speed of reconfiguration algorithms (Velasco et al., 2005). As discussed in Storey et al. (2013) the architecture should be optimized in real time. In Velasco-Quesada et al. (2009) the authors introduced the

4	3	4	1
4	4	1	3
3	2	4	3
1	3	4	4
Matrix M			

170	200	250	490
520	680	480	640
720	410	550	290
150	830	140	180
Starting Matrix P			

170	200	250		640	410
520	680	480			
720			290	180	490
150	830	140		550	
Resulting Matrix					

Fig. 18. Comparison between the starting and the resulting configuration.

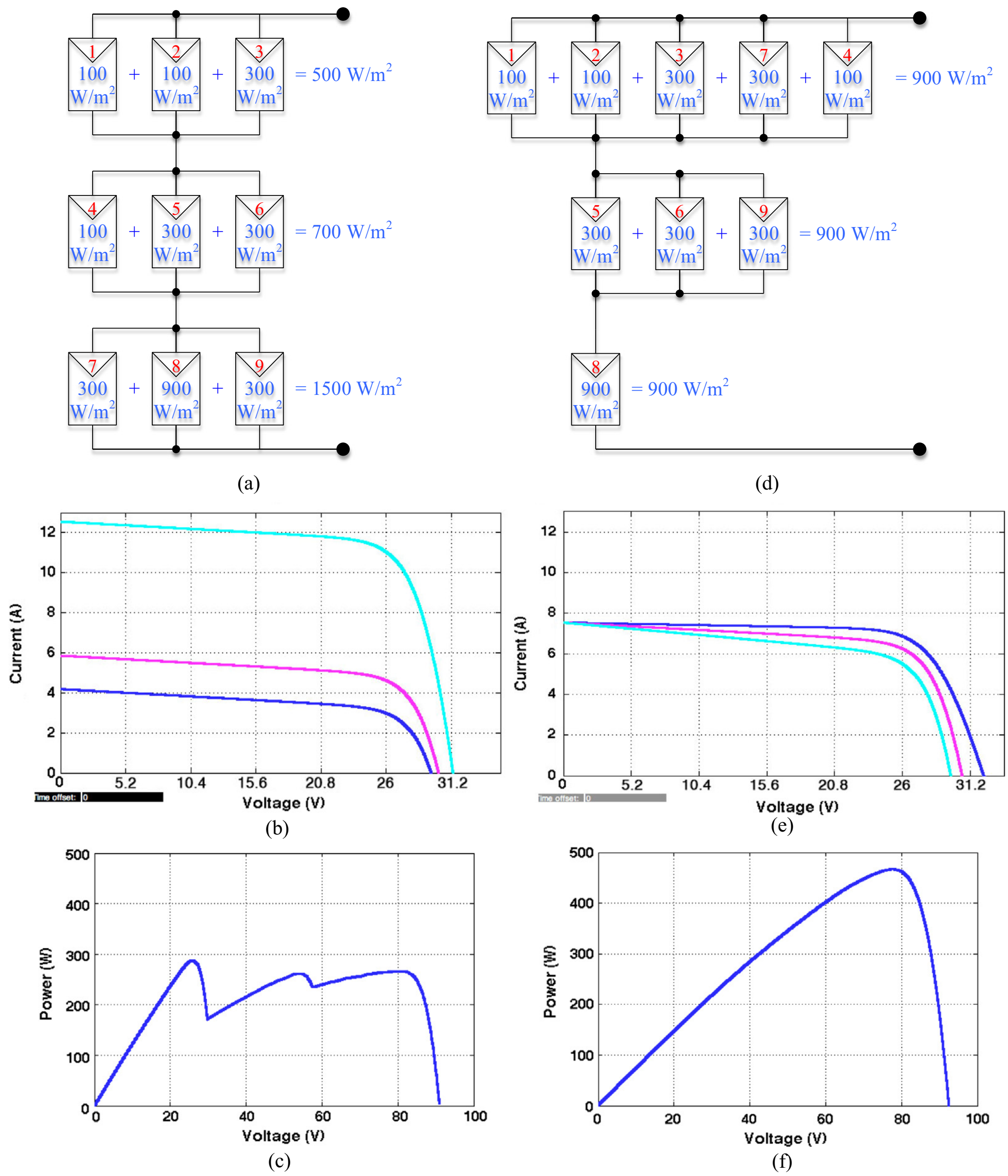

Fig. 20. Pv system before reconfiguration (a, b, c) and after reconfiguration with equalization DES (d, e, f).

Table 2
Comparison of reconfiguration algorithms for TCT arrays (A2.3).

Method	Authors	Speed	Optimal result	Not-equal rows	Preserving aging
SSP/MAA	Riva Sanseverino et al.	Fast	Sub-optimal	Yes	Yes
EAR PV	Velasco-Quesada et al. (2009)	Slow	Optimal	No	No
BWSA	Storey et al. (2013)	Fast	Sub-optimal	No	No
RSA	Romano et al. (2013)	Fast	Sub-optimal	Yes	No
Deterministic	Romano et al. (2013)	Slow	Optimal	Yes	No

irradiance equalization algorithm; in their work they compute the configurations of interest in order to reduce the complexity of the switching matrix. The time need for the reconfiguration was reported as 200 ms for a 6-cell array using the EAR algorithm. For bigger arrays the needed time can increase up to hours. The algorithm proposed in

Storey et al. (2013) – BWSA – is an iterative and hierarchical sorting algorithm that is designed to establish a near optimum configuration within a small number of iterations. The BWSA is very fast but its results are not optimal in most cases. As an example, in Fig. 22, the application steps of the BWSA are reported. It is easy to observe that

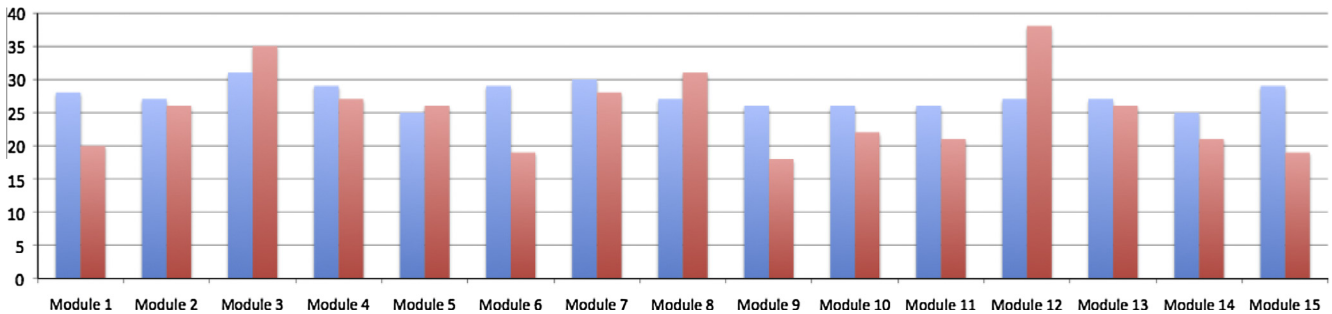

Fig. 21. Comparison of aging equalization (blue) versus the minimizing of the global switching operations (red). (For interpretation of the references to color in this figure legend, the reader is referred to the web version of this article.)

170	200	250	490
520	680	480	640
720	410	550	290
150	830	140	180

Initial matrix

830	720	680	640
550	520	490	480
410	290	250	200
180	170	150	140

1st step: order the matrix

830	720	680	640
480	490	520	550
410	290	250	200
140	150	170	180

2nd step: flip even rows

1310	1210	1200	1190
550	440	420	380

4st step: add I-II and III-IV rows

1310	1210	1200	1190
380	420	440	550

5th step: flip even row

1690	1630	1640	1740

6th step: add I-II rows

Fig. 22. Example of the best worst sorting algorithm.

the results obtained applying the two algorithms are as follows:

$$\mathrm{EI}_{\mathrm{new\_algorithm}} = 1680 - 1670 = 10$$

$$\mathrm{EI}_{\mathrm{BWSA}} = 1740 - 1630 = 110$$

In Romano et al. (2013), the authors introduce two different reconfiguration control algorithms for TCT architectures and using the irradiance equalization principle: a random search and a deterministic algorithm. The solution method builds rows with a non-equal number of modules, thus the number of possible interconnection configurations increases. The deterministic algorithm obtains the best configuration in higher time than the one needed by the RSA Romano et al. (2013).

An important feature of some approaches is also the ability of the switching matrix and of the algorithm to obtain a solution having rows with a non-equal number of modules, thus increasing the number of possible interconnection configuration, as in Romano et al. (2013).

So far, the algorithms here introduced only refer to "irradiance equalization" without accounting for switches aging and switching operations balancing. On the contrary, the proposed algorithm obtains the minimization of switching operation by means of the MAA and another post-processing algorithm allows choosing the solution providing a balanced solution, in terms of aging of switches.

6.1. Processing speed

The used Dynamic Programming for Subset-Sum problem make the time and space complexity for g modules with m rows with a P total irradiation is thus $O(mgP)$ (Silvano Martello, 1990), it takes maximum 30.72 ms of CPU time with a microprocessor 2.5 Ghz with Intel Core i5 to calculate the arrangement of a 16-cell array and reconfiguration with 4 rows. The MAA solves the assignment problem in $O(n^3)$ time (Munkres, 1957); it takes maximum 0.122 ms for 16-cell array.

Calculation times compared to the dynamics of weather phenomena is still quite limited, thus giving rise to a quasi real time operation. In the Palermo (Italy) area, as an example, the average maximum wind speed (averaged in the last ten years) is of 6.4 m/s. This means that with PV generators having extensions of tens of meters, the passage of clouds, in the worst situations, can occur in a few seconds which is a time much larger than the above cited computation time. Mechanical switching time is also very limited to a few ms, thus giving rise to a simple system to implement optimal reconfiguration systems.

7. Conclusion

In this paper, a new algorithm for optimized PV modules reconfiguration maximizing the performances of a PV generator in both shading conditions and non-uniform aging of the modules has been presented. The reconfiguration is here referred to the TCT connection and to the well known irradiance equalization principle.

The representation of the problem as a Subset-Sum problem and the idea to apply then the MAA to obtain the sub-optimal final configuration allows to obtain also the configuration that give rise to a minimum number of switching operations. A post-processing module stores a few comparable configurations (in terms of irradiance equalization) and allows to choose also the best configuration in terms of aging balancing. Future work is addressed on solving the problem of balancing the switching operations depending on the current that passes through the relays. In detail, it will be considered that a relay passed through by a current x-times lower than the maximum possible current value can consume the relay lifetime x-times less. Therefore, in that case the switching operation will not be considered as one switching operation but rather as a fraction of a switching operation.

References

Achim Woytea, J.N., Belmans, Ronnie, 2003. Partial shadowing of photovoltaic arrays with different system configurations: literature review and field test results. Solar Energy 74, 17.

Candela, R. et al., 2012. A Dynamic Electrical Scheme for the Optimal Reconfiguration of PV Modules Under Non-homogeneous Solar Irradiation. Trans Tech Publications, Switzerland, p. 197.

El-Dein, M.Z.S., Kazerani, M., Salama, M.M.A., 2011. Novel configurations for photovoltaic farms to reduce partial shading losses. Power and Energy Society General Meeting, 2011 IEEE, p. 1–5.

El-Dein, M.Z.S., Kazerani, M., Salama, M.M.A., 2012. Optimal photovoltaic array reconfiguration to reduce partial shading losses. IEEE Trans. Sustain. Energy 4 (1), 9.

Electricity from Sunlight, 2011. Electricity from Sunlight: An Introduction to Photovoltaics. Choice: Current Reviews for Academic Libraries 48 (5), p. 933–933.

La Manna, Damiano, Li Vigni, Vincenzo, Riva Sanseverino, Eleonora, Di Dio, Vincenzo, Romano, Pietro, 2014. Reconfigurable electrical interconnection strategies for photovoltaic arrays: a review. Renew. Sustain. Energy Rev.

Liu, Yi-Hua, Chen, Jing-Hsiao, Huang, Jia-Wei, 2014. Global maximum power point tracking algorithm for PV systems operating under partially shaded conditions using the segmentation search method. Solar Energy 103 (May), 350–363.

Lorente, Daniel Gómez, Pedrazzi, Simone, Zini, Gabriele, Rosa, Alberto Dalla, Tartarini, Paolo, 2014. Mismatch losses in PV power plants. Solar Energy 100, 42–49.

MacKay, D.J., 2009. In: Sustainable Energy – Without the Hot Air, vol. 2010. UIT Cambridge.

Munkres, J., 1957. Algorithms for assignment and transportation problems. J. Soc. Indust. Appl. Math. 5.

Nguyen, D., Lehman, B., 2008. An adaptive solar photovoltaic array using model-based reconfiguration algorithm. IEEE Trans. Indust. Electron. 55 (7), 2644–2654.

Picault, D., Raison, B.B., Aguilera, S., De La Casa, J., 2010. Changing photovoltaic array interconnections to reduce mismatch losses: a case study. In: 9th International Conference on Environment and Electrical Engineering (EEEIC), 2010, p. 37–40.

Quaschning, V., Hanitsch, R., 1996. Influence of shading on electrical parameters of solar cells. In: Conference Record of the Twenty Fifth IEEE Photovoltaic Specialists Conference – 1996, p. 1287–1290.

Ramabadran, R., 2009. Effect of shading on series and parallel connected solar PV modules. Modern Appl. Sci. 3.

Ramaprabha, R.M.B., 2012. A comprehensive review and analysis of solar photovoltaic array configurations under partial shaded conditions. Int. J. Photoenergy, 16.

Ramaprabha, R., Mathur, B.L., 2008. Modelling and simulation of Solar PV Array under partial shaded conditions. In: IEEE International Conference on Sustainable Energy Technologies, 2008. ICSET, pp. 7–11.

Ramaprabha, R., Mathur, B., Murthy, M., Madhumitha, S., 2010. New configuration of solar photo voltaic array to address partial shaded conditions. In: 3rd International Conference on Emerging Trends in Engineering and Technology (ICETET), 2010, p. 328–333.

Rauschenbach, H.S., 1971. Electrical output of shadowed solar arrays. IEEE Electron. Dev. Soc. (August), 483–490

Romano, P., Candela, R., Cardinale, M., Li Vigni, V., Musso, D., Riva Sanseverino, E., 2013. Optimization of photovoltaic energy production through an efficient switching matrix. J. Sustain. Develop. Energy, Water Environ. Syst. 1 (3), 227–236.

Silvano Martello, P.T., 1990. Subset-sum problem. Ebook – Knapsack Problems – Algorithms and Computer Implementations, pp. 105–130.

Storey, J.P., Wilson, P.R., Bagnall, D., 2013. Improved optimization strategy for irradiance equalization in dynamic photovoltaic arrays. IEEE Trans. Power Electron. 28 (6), 2946–2956. http://dx.doi.org/10.1109/TPEL.2012.2221481.

Swaleh, M.S., 1982. Effect of shunt resistance and bypass diodes on the shadow tolerance of solar cell modules. Solar Cells 5 (2), 183–198.

Tian, Hongmei, Mancilla-David, Fernando, Ellis, Kevin, Muljadi, Eduard, Jenkins, Peter, 2013. Determination of the optimal configuration for a photovoltaic array depending on the shading condition. Solar Energy 95 (September), 1–12.

Trends in Photovoltaic Applications, 2013. Trends in Photovoltaic Applications. Survey report of selected IEA countries between 1992 and 2012. International Energy Agency.

Velasco, G., Negroni, J.J., Guinjoan, F., Piqué, R., 2005. Irradiance equalization method for output power optimization in plant oriented grid-connected PV generators. In: European Conference on Power Electronics and Applications, 2005, p. 10.

Velasco-Quesada, G. et al., 2009. Electrical PV array reconfiguration strategy for energy extraction improvement in grid-connected PV systems. IEEE Trans. Indust. Electron. 56 (11), 4319–4331.

Villa, Luiz Fernando Lavado et al., 2012. Maximizing the power output of partially shaded photovoltaic plants through optimization of the interconnections among its modules. Photovoltaics IEEE J. of 2.2, 154–163.